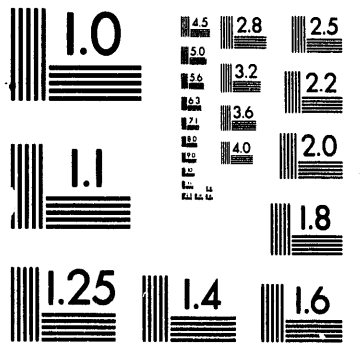
1.0
1.1
1.25
1.4
1.6
1.8
2.0
2.2
2.5
2.8
3.2
3.6
4.0
4.5
5.0
5.6
6.3
7.1
8.0
9.0

1 of 1

Final Report:

Large Eddy Simulations using Lattice Boltzmann Algorithms

September 28,1993

James D. Sterling
Principal Investigator

Sponsored by:
Los Alamos National Laboratory
Theoretical Division

Contract # 9-XA3-1425E

DISCLAIMER

This report was prepared as an account of work sponsored by an agency of the United States Government. Neither the United States Government nor any agency thereof, nor any of their employees, makes any warranty, express or implied, or assumes any legal liability or responsibility for the accuracy, completeness, or usefulness of any information, apparatus, product, or process disclosed, or represents that its use would not infringe privately owned rights. Reference herein to any specific commercial product, process, or service by trade name, trademark, manufacturer, or otherwise does not necessarily constitute or imply its endorsement, recommendation, or favoring by the United States Government or any agency thereof. The views and opinions of authors expressed herein do not necessarily state or reflect those of the United States Government or any agency thereof.

RECEIVED
JAN 27 1994
OSTI

MASTER

DISTRIBUTION OF THIS DOCUMENT IS UNLIMITED

Abstract

This report contains the results of a study performed to implement eddy-viscosity models for Large-Eddy-Simulations (LES) into Lattice Boltzmann (LB) algorithms for simulating fluid flows. This implementation requires modification of the LB method of simulating the incompressible Navier-Stokes equations to allow simulation of the filtered Navier-Stokes equations with some subgrid model for the Reynolds stress term. We demonstrate that the LB method can indeed be used for LES by simply locally adjusting the value of the BGK relaxation time to obtain the desired eddy-viscosity. Thus, many forms of eddy-viscosity models including the standard Smagorinsky model or the Dynamic model may be implemented using LB algorithms. Since underresolved LB simulations often lead to instability, the LES model actually serves to stabilize the method. An alternative method of ensuring stability is presented which requires that entropy increase during the collision step of the LB method. Thus, an alternative collision operator is locally applied if the entropy becomes too low. This stable LB method then acts as an LES scheme that effectively introduces its own eddy viscosity to damp short wavelength oscillations.

Contents

List of Figures

Chapter 1

Introduction

This report describes a three-month effort whose objectives were to incorporate eddy-viscosity models for Large-Eddy-Simulation into Lattice Boltzmann computer codes and to perform numerical simulations using the methods for comparison with traditional CFD results. The report describes the accomplishment of these objectives and concludes with some recommendations for future work.

Numerical simulations of turbulent fluid flow in non-trivial geometries are almost always "underresolved". This is because the speed and memory of current computational facilities do not allow resolution of all of the scales of turbulence. Thus, fluids simulations make use of some type of subgrid model to include the physical effect that the unresolved motions have on the resolved fluid motion. These models often take the form of eddy-viscosity models for the Reynolds stresses that serve to damp oscillations of short wavelength. Recent research at Stanford's Center for Turbulence Research has demonstrated that in some turbulent flows, the eddy-viscosity acting on scales smaller than some applied test grid is a large positive number at some locations and is a large negative number at others, at a given time[1]. Averaging over time, there is net dissipation that corresponds to a positive average subgrid viscosity.

Thus the standard Smagorinsky model, which always makes use of a positive eddy viscosity, does not adequately represent the "backscatter" that occurs when energy flows from small scales to the larger scales of fluid motion. While the eddy-viscosity models appear to be "physical" subgrid models, Boris[2] has argued that any stable numercial method applied to the Navier-Stokes equations implicitly contains a subgrid model because short wavelength oscillations are damped. Indeed, if one uses a stable scheme in conjunction with a Smagorinsky-type model, it is not possible to distinguish between the effects of eddy-viscosity and numerical viscosity of the method.at short wavelengths.

This issue of subgrid physics vs. numerical stability is the primary debate currently underway in the turbulence simulation community. Can the physics of energy exchange between resolved and unresolved scales be adequately modelled or can a stable numerical scheme do as well? The work presented in this report does not presume to take sides in this debate but simply demonstrates that the Lattice Boltzmann (LB) computational method is amenable to either approach.

The LB method of simulating laminar fluid flows has been demonstrated to be a

numerically efficient and accurate alternative to other numerical methods. However, underresolved LB simulations often lead to instability. Inclusion of an eddy-viscosity model is shown to stabilize LB simulations of 3-d channel flow. Alternatively, since more standard CFD methods lead to unphysical dissipation at short wavelength, one may similarly stabilize LB methods by defining an entropy-increasing collsion operator that is applied only when the local entropy becomes too small. If the fraction of sites at which this collision operator is applied remains small then Navier-Stokes behavior should be accurately simulated for the longer wavelengths.

In Chapter 2, a derivation of the LB long-wavelength, low-frequency behavior is derived and the modifications necessary to implement both the Smagorinsky-type models and the entropy-increasing collision are presented. In Chapter 3 the results of some 3-d channel flow simulations are presented. Chapter 4 presents some conclusions and recommendations for future work.

Chapter 2

Theory of Turbulent Flow Simulation

2.1 Review of Chapman-Enskog Method

This section provides a description of the Chapman-Enskog expansion applied to the Boltzmann equation with the following definitions and conditions: 1) The particle populations f may only move with velocities that are members of the set of discrete velocity vectors e_i. The corresponding populations are denoted f_i. 2) A collision operator with a single relaxation time, τ, is used to redistribute populations f_i towards equilibrium values f_i^{eq}. This is also referred to as a BGK collision operator where τ is inversely proportional to density [3]. For constant density flows τ is a constant. 3) The equilibrium velocity distribution function is written as a truncated power series in the macroscopic flow velocity.

The discrete velocity Boltzmann equation then becomes

$$\frac{\partial f_i}{\partial t} + \mathbf{e}_i \cdot \nabla f_i = -\frac{1}{\tau}(f_i - f_i^{eq}) \tag{2.1}$$

where the velocity distribution function f_i is constructed so that macroscopic flow variables are defined by its moments: Mass:

$$n \equiv \sum_i f_i \tag{2.2}$$

Momentum:

$$n\mathbf{u} \equiv \sum_i f_i \mathbf{e}_i \tag{2.3}$$

Equation (2.1) may be written in non-dimensional form by using a characteristic flow length scale L, reference speed e_r, and density n_r. Two reference time scales are used, t_c to represent the time between particle collisions and L/e_r to represent a characteristic flow time. The reference speed may be selected to be the magnitude of the minimum non-zero discrete velocity. If only one speed is used, then the velocity set for the non-dimensional equations is simply a set of unit vectors. The resulting

non-dimensional equation is

$$\frac{\partial \hat{f}}{\partial \hat{t}} + \hat{\mathbf{e}}_i \cdot \hat{\nabla} \hat{f} = -\frac{1}{\varepsilon \hat{\tau}} (\hat{f} - \hat{f}^{eq}) \tag{2.4}$$

where the caret symbol is used to denote non-dimensional quantities $\hat{\mathbf{e}}_i = \mathbf{e}_i / e_r, \hat{\nabla} = L\nabla$, $\hat{t} = te_r/L$, $\hat{\tau} = \tau/t_c$, and $\hat{f} = f_i/n_r$. The parameter $\varepsilon = t_c e_r / L$ and may be interpreted as either the ratio of collision time to flow time or as the ratio of mean free path to the characteristic flow length (i.e. Knudsen number). We will not use the caret notation further but will assume that the equations are in non-dimensional form henceforth.

The first step in the Chapman-Enskog procedure is to invoke a multi-scale expansion of the time and space derivatives in the small parameter, ε as follows.

$$\frac{\partial}{\partial t} = \frac{\partial}{\partial t_1} + \varepsilon \frac{\partial}{\partial t_2} + ... \tag{2.5}$$

$$\nabla = \nabla_1 + \varepsilon \nabla_2 + ... \tag{2.6}$$

We also expand the distribution function as

$$f_i = f_i^{(0)} + \varepsilon f_i^{(1)} + \varepsilon^2 f_i^{(2)} + ... \tag{2.7}$$

where the zeroth-order term is the equilibrium distribution function so that the collision operator becomes

$$-\frac{1}{\varepsilon \tau}(f_i - f_i^{eq}) = -\frac{1}{\tau}(f_i^{(1)} + \varepsilon f_i^{(2)} + ...). \tag{2.8}$$

Since mass and momentum are conserved in collisions, the sum over the i velocities of the collision term and the collision term multiplied by $\mathbf{e}_i$ must be zero. Therefore, the sums on f_i in equations (2.2) and (2.3) also hold for $f_i^{(0)}$ and sums over nonequilibrium populations are zero. We make the further assumption that sums over the nonequilibrium populations corresponding to each order in ε independently vanish: $\sum_i f_i^{(l)} = 0$ and $\sum_i \mathbf{e}_i f_i^{(l)} = 0$ for $l > 0$.

Substituting the above expansions into the Boltzmann equation, we obtain equations of zeroth and first order in ε which are written separately as

$$\frac{\partial}{\partial t_1} f_i^{(0)} + \mathbf{e}_i \cdot \nabla_1 f_i^{(0)} = -\frac{1}{\tau} f_i^{(1)} \tag{2.9}$$

and

$$\frac{\partial}{\partial t_2} f_i^{(0)} + \frac{\partial}{\partial t_1} f_i^{(1)} + \mathbf{e}_i \cdot \nabla_1 f_i^{(1)} + \mathbf{e}_i \cdot \nabla_2 f_i^{(0)} = -\frac{1}{\tau} f_i^{(2)} \tag{2.10}$$

where it has been assumed that τ is $O(1)$.

When equations (2.9) and (2.10) are summed over the i velocities the continuity or mass conservation equation to first order in ε is obtained as

$$\frac{\partial n}{\partial t} + \nabla \cdot (n\mathbf{u}) = 0. \tag{2.11}$$

The momentum equation to first order in ϵ is obtained by multiplying the above equations by $\mathbf{e}_i$ and then summing over velocities to obtain,

$$\frac{\partial}{\partial t}(n\mathbf{u}) + \nabla \cdot (\mathbf{\Pi}^{(0)} + \mathbf{\Pi}^{(1)}) = 0 \tag{2.12}$$

where $\mathbf{\Pi}^{(l)}$ is the momentum flux tensor and is defined as

$$\mathbf{\Pi}^{(l)}_{\alpha\beta} = \sum_i e_{i\alpha} e_{i\beta} f_i^{(l)} \tag{2.13}$$

for $l = 0, 1$. The constitutive relations for this tensor are obtained by selecting a particular lattice geometry and equilibrium distribution functional form and then proceeding to match moments of the distribution function with terms in the Navier-Stokes equations.

As an example, when this is performed for a hexagonal lattice with unit velocity vectors defined by $\mathbf{e}_i = \{cos(2\pi(i-1)/6), sin(2\pi(i-1)/6)\}$ for i =1,2,...,6, a suitable equilibrium distribution function is found to be

$$f_0^{eq} = n\alpha - nu^2 \tag{2.14}$$

$$f_i^{eq} = \frac{n(1-\alpha)}{6} + \frac{n}{3}\mathbf{e}_i \cdot \mathbf{u} + \frac{2n}{3}(\mathbf{e}_i \cdot \mathbf{u})^2 - \frac{n}{6}u^2 \tag{2.15}$$

where α is a constant that determines the distribution of mass between the moving and nonmoving populations [4].

We may readily evaluate the constitutive relations for this distribution function by making use of the lattice relations

$$\sum_i e_{i\alpha} e_{i\beta} = 3\delta_{\alpha\beta} \tag{2.16}$$

$$\sum_i e_{i\alpha} e_{i\beta} e_{i\gamma} e_{i\theta} = \frac{3}{4}(\delta_{\alpha\beta}\delta_{\gamma\theta} + \delta_{\alpha\gamma}\delta_{\beta\theta} + \delta_{\alpha\theta}\delta_{\beta\gamma}), \tag{2.17}$$

and noting that summations of an odd number of e_i's are equal to zero.

Substituting equation (2.15) into the equation (2.13) for $\mathbf{\Pi}^{(l)}$ above, we find that

$$\mathbf{\Pi}^{(0)}_{\alpha\beta} = 3n\frac{1-\alpha}{6}\delta_{\alpha\beta} + nu_\alpha u_\beta \tag{2.18}$$

which gives a Galilean invariant convective term in the momentum equation. By identifying the isotropic part of this tensor as the pressure, we obtain an ideal gas law equation of state (i.e. $p = \frac{1-\alpha}{2}n$) and the gradient of the pressure in the momentum equation. The other term in the momentum equation is obtained by using Equation (2.9) as an expression for $f_i^{(1)}$ to obtain

$$\mathbf{\Pi}^{(1)}_{\alpha\beta} = -\tau\{\frac{\partial}{\partial t}\mathbf{\Pi}^{(0)}_{\alpha\beta} + \frac{\partial}{\partial x_\gamma}\sum_i e_{i\alpha} e_{i\beta} e_{i\gamma} f_i^{(0)}\}. \tag{2.19}$$

The next step in the Chapman-Enskog procedure is to replace time derivatives at this order ε level with spatial derivatives using the Euler level equations. Thus, the time derivative of the density in the above equation may be replaced using the continuity equation. Also, the time derivative of $nu_\alpha u_\beta$ can be replaced using the Euler level momentum equation which converts the time derivative to spatial derivatives as follows

$$\frac{\partial}{\partial t}(nu_\alpha u_\beta) = u_\alpha(-\frac{\partial p}{\partial x_\beta} - nu_\alpha\frac{\partial u_\beta}{\partial x_\alpha}) + u_\beta(-\frac{\partial p}{\partial x_\alpha} - \frac{\partial}{\partial x_\beta}(nu_\alpha u_\beta)) \tag{2.20}$$

where the terms of $O(u^3)$ are neglected in the incompressible limit. The equation of state from equation (2.18) is used to replace the pressure gradient with a density gradient. Finally, when the equilibrium distribution is substituted into the last term of equation (2.19), the only term that remains is the $\mathbf{e}_i \cdot \mathbf{u}$ term which is evaluated using Equation (2.17).

Upon substitution into equation (2.12), the final form of the momentum equation is

$$n\frac{\partial u_\alpha}{\partial t} + nu_\beta\frac{\partial u_\alpha}{\partial x_\beta} = -\frac{\partial p}{\partial x_\alpha} + \frac{\partial}{\partial x_\beta}(\frac{\lambda}{n}(\frac{\partial nu_\gamma}{\partial x_\gamma} + u_\alpha\frac{\partial n}{\partial x_\beta} + u_\beta\frac{\partial n}{\partial x_\alpha})) + \frac{\partial}{\partial x_\beta}(\mu(\frac{\partial u_\beta}{\partial x_\alpha} + \frac{\partial u_\alpha}{\partial x_\beta})) \tag{2.21}$$

where

$$\mu = \frac{\tau n}{4} \tag{2.22}$$

and

$$\lambda = \frac{\tau n(2\alpha - 1)}{4}. \tag{2.23}$$

In two dimensions, the bulk viscosity is the sum of these two so that

$$K = \frac{\tau n\alpha}{2} \tag{2.24}$$

which gives zero bulk viscosity as expected for the monatomic gas when energy is conserved (i.e. when $\alpha = 0$ it can be shown that conservation of mass is equivalent to conservation of energy).

Note that these equations are not the standard Navier-Stokes equations because there are derivatives of the density in the second viscosity term on the right side of the equation. If these gradients of density are negligible this hexagonal lattice, discrete Boltzmann equation should behave approximately as the Navier-Stokes equations. Since the gradients of the density are $O(u^2)$ (see references [5] and [6]), the unphysical terms in equation (2.21) are $O(u^3)$. Thus, although the physics contains compressibility effects (that differ from the compressible Navier-Stokes equations), one may come arbitrarily close to solving incompressible flow by reducing the Mach number and thereby allowing information to propagate throughout the domain while little convection occurs. For this reason, no Poisson solver is required to determine the pressure and simple particle reflections at boundaries may be used to invoke no-slip conditions. We also note that if the second viscosity λ is zero, the complete compressible Navier-Stokes equations are given but the bulk viscosity is then nonzero.

There are differences between the incompressible Navier-Stokes equations and the macroscopic behavior of the discrete-velocity Boltzmann equations because of the asymptotic nature of the Chapman-Enskog method. The differences may be attributed to Burnett level and higher level terms or as small deviations from the above relation for the kinematic viscosity. For this reason, previous LB studies have reported comparisons between the Chapman-Enskog prediction and numerical simulation measurements of the viscosity (e.g. Kadanoff et. al. [7]). However, the Burnett level terms are expected to become negligible as the global Knudsen number becomes small. Since the Knudsen number is proportional to the Mach number divided by the Reynolds number, the Burnett terms may be classified with other "compressibility" effects and should become small as the Mach number approaches zero for a fixed Reynolds number.

In conclusion, the discrete Boltzmann equation in dimensionless form, equation (2.4), may be discretized and numerically simulated to provide approximate solution to the continuity and momentum equations given by equations (2.11) and (2.21), respectively. The results can then be put back into dimensional form using the reference quantities. Simulations may come arbitrarily close to incompressible Navier-Stokes behavior with differences being attributed solely to discretization and compressibility effects.

2.2 The Lattice Boltzmann Discretization

At this point we will narrow our view to a particular discretization of the non-dimensional discrete Boltzmann equation. In particular, we will choose the lattice-Boltzmann method which is an exact Lagrangian solution for the convective derivatives. For a given convection velocity, this type of scheme is typically obtained by using an Euler time step in conjunction with an upwind spatial discretization and then setting the grid spacing divided by the time step equal to the velocity. Discretization of equation (2.4) results in the following equation.

$$\frac{f_i(\mathbf{x}, t+\Delta t) - f_i(\mathbf{x}, t)}{\Delta t} + \frac{f_i(\mathbf{x}+\mathbf{e}_i\Delta x, t+\Delta t) - f_i(\mathbf{x}, t+\Delta t)}{\Delta x} = -\frac{(f_i(\mathbf{x}, t) - f_i^{(0)}(\mathbf{x}, t))}{\epsilon\tau}. \tag{2.25}$$

Lagrangian behavior is then obtained by the selection of the lattice spacing divided by the time step to equal the magnitude of $\mathbf{e}_i$, which was normalized so that the smallest velocity magnitude is unity. When the equation is multiplied by Δt, the result is the cancellation of two terms on the left side of the above equation leaving only one term evaluated at $t + \Delta t$ so that the method is explicit. The next characteristic of the lattice Boltzmann method is the selection of the time step to equal the reference collision time. The result is the cancellation of the Knudsen number in the denominator of the collision term giving the following simple form that is commonly referred to as the lattice Boltzmann equation (LBE).

$$f_i(\mathbf{x} + \mathbf{e}_i\Delta t, t + \Delta t) - f_i(\mathbf{x}, t) = -\frac{1}{\tau}(f_i(\mathbf{x}, t) - f_i^{(0)}(\mathbf{x}, t)). \tag{2.26}$$

This equation has a particularly simple physical interpretation in which the collision term is evaluated locally and there is only one streaming step or "shift" operation per lattice velocity. This stream-and-collide particle interpretation is a result of the fully-Lagrangian character of the equation for which the lattice spacing is the distance travelled by the particles during a time step. Higher order discretizations of the discrete Boltzmann equation typically require several "shift" operations for the evaluation of each derivative and a particle interpretation is less obvious. In fact, the entire derivation of the LB method was originally based on the idea of generalizing LG models by solving the LG Boltzmann equation and relaxing the exclusion principle that particle populations be either zero or one for each velocity [8]. It did not originally occur to the authors that the LB method could be considered a particular discretization for the discrete Boltzmann equation.

The particle model allows boundary conditions to be implemented as particular types of collisions. If populations are reflected directly back along the lattice vector along which they streamed, the result is a "no-slip" velocity boundary condition. One may also define specular reflection conditions that yield a slip condition. Models for which energy is conserved allow specification of heat-transfer boundary conditions using particle reflection conditions as well [9]. These simple boundary conditions make the LB method particularly suited to parallel computing environments and the simulation of flows in complex geometries.

Although first order discretizations have been used, the LB method is typically considered to be a second order method because contributions that result from discretization error are taken to represent physics [10]. The inclusion of numerical viscosity is accomplished by Taylor expanding equation (2.26) about x and t. When the second order terms in this expansion are included in the above Chapman-Enskog analysis, the result is that the coefficient τ in the transport coefficients is simply replaced by $\tau - \frac{1}{2}$ (see reference [9]). Thus, the lattice contribution to the viscosity for this LB scheme is negative, requiring the value of the relaxation time to be greater than half of the time step to maintain positive viscosity. Note that third-order terms in the Taylor-series expansion are necessarily of order ϵ^3 in the Chapman-Enskog expansion. Thus, as with traditional kinetic theory, there may be some error arising from the Burnett level terms.

Since the LB method under consideration is valid only in the incompressible limit, the main dimensionless parameter of interest is the Reynolds number. Convergence of the solution to the incompressible Navier-Stokes equations for a fixed Reynolds number is then obtained by letting the Mach number become small enough to remove compressibility effects, and letting the lattice spacing $\mathbf{e}_i\Delta t$ become small enough to "resolve" the flow. Reverting to the caret notation for dimensionless quantities, the Reynold's number for the hexagonal lattice may now be written

$$Re = \frac{LU}{\nu} = \frac{4N\hat{U}}{\hat{\tau} - \frac{1}{2}}. \tag{2.27}$$

where $N = \frac{L}{\Delta x}$ is the number of lattice spaces. The dimensionless velocity is the characteristic Mach number which should be small to simulate incompressible flow.

Thus, the convergence at a given Reynolds number is performed by increasing N while either increasing $\hat{\tau}$ and/or decreasing $\hat{U}$ appropriately. For a decrease in the value of $\hat{U}$, a proportionate increase in the number of time steps is needed to reach the same flow evolution time.

Concluding, the LB method makes use of first order discretizations of the dimensionless discrete velocity Boltzmann equation in both time and space. The dimensionless time step and lattice spacing are set equal and numerical contributions to viscosity are accounted for and considered to be part of the physics of the method. With these effects included, the LB method is a second order method in both space and time for the simulation of the Navier-Stokes equations. In the use of LB models developed for incompressible Navier-Stokes simulation care must be taken to ensure that both the Mach number and the Knudsen number are small enough that the deviation from incompressible behavior is negligible.

2.3 Large-Eddy Simulations

In the simulation of any fluid flow, a discrete grid and time step are used so that the desired results of the computation are not simply the values of the independent variables of the corresponding governing PDE's at the grid points at each time step. On the contrary, since the grid and time step limit the results to a finite range of wavenumbers and frequencies, the computational results desired are those of a filtered version of the governing PDE's. The large-scale quantities one would like to simulate are defined by a filtering operation

$$\overline{f}(x) = \int f(x)\, G(x, x')\, dx' \tag{2.28}$$

where G is the filter function and the integral is extended over the entire domain. Several different filters are used which depend on the numerical method in use. For finite difference methods, the box filter is used (whether one acknowledges its existence or not!) and is defined as follows

$$G_i(x_i, x_i') = \begin{array}{l} \frac{1}{\Delta_i} \text{ for } |x_i - x_i'| < \frac{\Delta_i}{2} \\ 0 \text{ otherwise,} \end{array} \tag{2.29}$$

while for spectral methods, a cutoff filter defined in Fourier space is

$$\widehat{G}_i(k_i) = \begin{array}{l} 1 \text{ for } k_i < K_i \\ 0 \text{ otherwise,} \end{array} \tag{2.30}$$

where $\widehat{G}_i$ is the Fourier coefficient of the filter function in the ith direction, G_i, $K_i = \pi/\Delta_i$ is the cutoff wavenumber, and $\Delta_i$is the filter width in the ith direction. The filtered continuity and Navier-Stokes equations are

$$\begin{aligned} \frac{\partial \overline{u}_i}{\partial x_i} &= 0 \\ \frac{\partial \overline{u}_i}{\partial t} + \overline{u}_j \frac{\partial \overline{u}_i}{\partial x_j} &= -\frac{1}{n} \frac{\partial \overline{p}}{\partial x_i} - \frac{\partial \tau_{ij}}{\partial x_j} + \frac{\partial}{\partial x_j} \left(\nu \left[\frac{\partial \overline{u}_i}{\partial x_j} + \frac{\partial \overline{u}_j}{\partial x_i} \right] \right). \end{aligned} \tag{2.31}$$

These equations govern the evolution of the resolved fluid motions. For laminar flows, today's computational power is often adequate to "resolve" the flow, which in the context of filtering simply means that the Reynolds stress term τ_{ij} is negligible. For turbulent flows however, the Reynolds stress

$$\tau_{ij} = \overline{u_i u_j} - \overline{u}_i \overline{u}_j \tag{2.32}$$

is significant and must be modeled in some way. The use of standard CFD methods applied to the Navier-Stokes equations, without this term being explicitly modeled, is equivalent to setting discretization error of the other terms equal to this Reynolds stress term. Thus, any numerical viscosity or other truncation error will effectively serve as a subgrid turbulence model. The main criterion for stability of numerical methods is that this term effectively damp short wavelength (but resolved) oscillations in the flow.

The most common approach of modeling is due to Smagorinsky [11] in which the anisotropic part of the Reynolds stress term is modeled as

$$\tau_{ij} - \frac{\delta_{ij}}{3}\tau_{kk} = -2\nu_t \overline{S}_{ij} = -2C\Delta^2 \left|\overline{S}\right| \overline{S}_{ij} \tag{2.33}$$

in which δ_{ij} is the Kronecker delta and $\left|\overline{S}\right| = \sqrt{2\overline{S}_{ij}\overline{S}_{ij}}$ is the magnitude of the large scale strain rate tensor

$$\overline{S}_{ij} = \frac{1}{2}\left(\frac{\partial \overline{u}_i}{\partial x_j} + \frac{\partial \overline{u}_j}{\partial x_i}\right). \tag{2.34}$$

and C is known as the Smagorinsky constant. The isotropic part of the Reynolds stress term is indistinguishable from the pressure term.

A popular recent modification to this model by Germano *et al* [12].is called the dynamic subgrid eddy viscosity model and applies a test filter in addition to the grid filter. The so-called "resolved Reynolds stress" terms that are computed for scales between the coarse test filter and the grid filter can then be used to locally compute the Smagorinsky constant, C. A problem with this model however is that the Smagorinsky constant may become locally negative and numerical instability ensues. This is avoided in practice by averaging over homogeneous flow planes to keep positive eddy viscosities. As mentioned in the introduction, the eddy-viscosity should indeed be negative for some time at some sites but should not lead to instability as observed numerically.

With this background in LES presented, how may LB methods be used to perform LES? The answer is that Equations 2.11 and 2.21 that are simulated using the LB method converge to equations 2.31 if the value of the collision relaxation time is locally adjusted so that the viscosity is equal to the sum of the physical and the eddy viscosities for the LES simulation as follows (e.g. for the hexagonal model presented in Section 2.1)

$$\nu_{LB} = \frac{\tau - \frac{1}{2}}{4} = \nu + C\Delta^2 \left|\overline{S}\right|. \tag{2.35}$$

Thus, the value of τ is locally adjusted depending on the local magnitude of the large scale strain rate tensor. The dynamic eddy viscosity model may also be implemented

by using the local value of C that is computed from the resolved Reynolds stress term using the applied test filter.

Concluding, the LB method may be used to perform LES simulations of turbulent fluid flow. Both the standard Smagorinsky model and the dynamic model of Germano *et al* [12]. have been implemented in Fortran computer programs and run on the CM-5 computer at the LANL Advanced Computing Laboratory.

2.4 Entropy-Increase Stability Method

As previously discussed, if standard CFD methods are applied to the Navier-Stokes equations, without subgrid stress modeling, then the discretization error serves as the subgrid model for the simulation. Since LB methods are notoriously unstable for underresolved simulations, the eddy-viscosity models presented in the previous section serve to stabilize the method by damping short wavelength oscillations that develop. Alternatively, since short-wavelength behavior needn't be "physical", we may locally stabilize the LB simulations other ways. Researchers have previously performed *ad hoc* procedures to stabilize the method but the results are seldom reported because the LB method has always been considered a "physical" model that should not require such tampering. One such procedure is to set particle populations equal to a small positive population if a collision indicates that negative populations should arise. This can be done in a manner that either conserves mass and momentum or does not. This locally "unphysical" tampering with the scheme may be the equivalent of introducing artificial viscosity or a subgrid eddy viscosity that damps short wavelength oscillations. We present here a potential method of stabilization of LB methods that may be somewhat more physically appealling than the *ad hoc* procedures just described.

As oscillations grow during an unstable LB simulation, the entropy decreases. One may therefore set a minimum entropy that is used to characterize numerical instability (or underresolution of the flow) and require that the entropy not decrease further. The entropy does not necessarily increase during an LB collision because in addition to conserving mass and momentum, additional constraints are imposed to guarantee that the governing equations are obtained in the long-wavelength limit. Since stability is desired for the short wavelength oscillations, if the entropy becomes too low, an alternative collision may be used which increases entropy while conserving mass and momentum.

We propose here that an entropy-increasing collision may be generated in one of the following three ways.

1) The method of Lagrangian multipliers may be used to determine the equilibrium distribution coefficients while mass and momentum are conserved but the other constraints may be temporarily relaxed. If there are few enough points in the flow, and for short enough time which reach the minimum entropy, then the long-wavelength Navier-Stokes behavior should be retained.

2) An apparently *ad hoc* approach is to use a collision that distributes the mass equally between all velocity states for zero velocity, that retains the coefficients on

the $e_i.u$ term that is normally used in the equilibrium distribution function, and that ignores higher order terms in the equilibrium distribution function. This should serve to locally increase the entropy while still conserving mass and momentum.

3) Finally, if a collision decreases the entropy below the minimum, then simply ignore the collision and go on to the streaming step. Since the mean free path is not inversely proportional to density in the LB method, the viscosity is proportional to the mean free path that is fixed by the lattice size. However, by ignoring a collision, the local mean free path is effectively increased and the corresponding local viscosity should increase and oscillations should be damped.

These methods have not been implemented into computer codes yet, it is proposed that future turbulence simulations that encounter instability when the flow becomes underresolved implement these three methods and compare results if stability is obtained.

Chapter 3

Channel Flow Simulations

Several simulations of channel flow were performed using LES models as described in Section 2.3. The 3-d LB method described by Alexander *et al.*[13] was used as the numerical scheme. A rectangular array of lattice sites was used with bounce-back particle reflection conditions at the top and bottom walls to provide a no-slip boundary condition. The front and back planes of the domain were connected so that periodicity in this direction was enforced (periodicity is automatically assumed by the CM-5 architecture). A linear pressure gradient was imposed in the flow direction and the velocity profiles were set to be initially parabolic at all axial locations. Two methods of simulation were then used. In the first method, the upstream velocity profile was set to be parabolic for all times and the downstream velocity gradient was set to zero. Simulations were performed until the downstream velocity reached a quasi-steady condition. The downstream conditions were then used as the upstream conditions and the flow was evolved until the downstream conditions again reached a quasi-steady flow. This was iterated to effectively simulate fully-developed flow conditions at different axial locations along the channel. The second method of simulation was to make the velocity periodic but to impose the pressure gradient as before. In this case, evolving the flow to quasi-steady state is performed and the simulation is stopped.

The first turbulence model implemented was the standard Smagorinsky eddy-viscosity model. As shown in Figure 1, if the Smagorinsky constant is set to zero, the flow reaches a laminar parabolic flow. The different curves represent iterations as discussed for the first method discussed in the previous paragraph. The figure sublabel indicates that 500 time steps were performed before the downstream conditions were moved to the upstream location and that this procedure was performed 10 times. Notice that even thought the Reynolds number was 6000, there were only four points in the transverse direction so that essentially no 3-d effects could be represented and transition to turbulence was not observed.

Figures 2 and 3 contain the results of simulations for which the x-direction and y-direction is more coarsely resolved but the z-resolution is finer than in the simulations described above. The mean flow velocity was obviously different for these to simulations. Additionally, "trip wires" two lattice sites tall were placed on two adjacent walls (spanning front and bottom walls) at a site 1/3 down the channel axis

and also on the other two walls (back and top walls) at a site 2/3 down the channel length. The result was the development of a numerical instability, the initial stages of which are seen in the figures.

The above simulations used zero eddy-viscosity. When the Smagorinsky constant was set to the usual value of 0.23, the numerical instability disappeared but the flow remained laminar with a non-parabolic velocity profile. This is consistent with the results of other Smagorinsky model simulations of transitional flow that are described by Piomelli *et al.*[1]. That is, the eddy-viscosity unphysically damps the oscillations that should develop, preventing the transition to turbulence from ever occurring. Others have observed transition by allowing oscillations to develop to a given amplitude before "turning-on" the eddy-viscosity. This *ad hoc* procedure is not very appealling and led to the development of the dynamic model that has its own numerical instability problems.

Transition to Turbulence in Channel Flow

Re=6000 nx=512 x 10 x 500 time steps ny=512 nz=4 τ=.5128

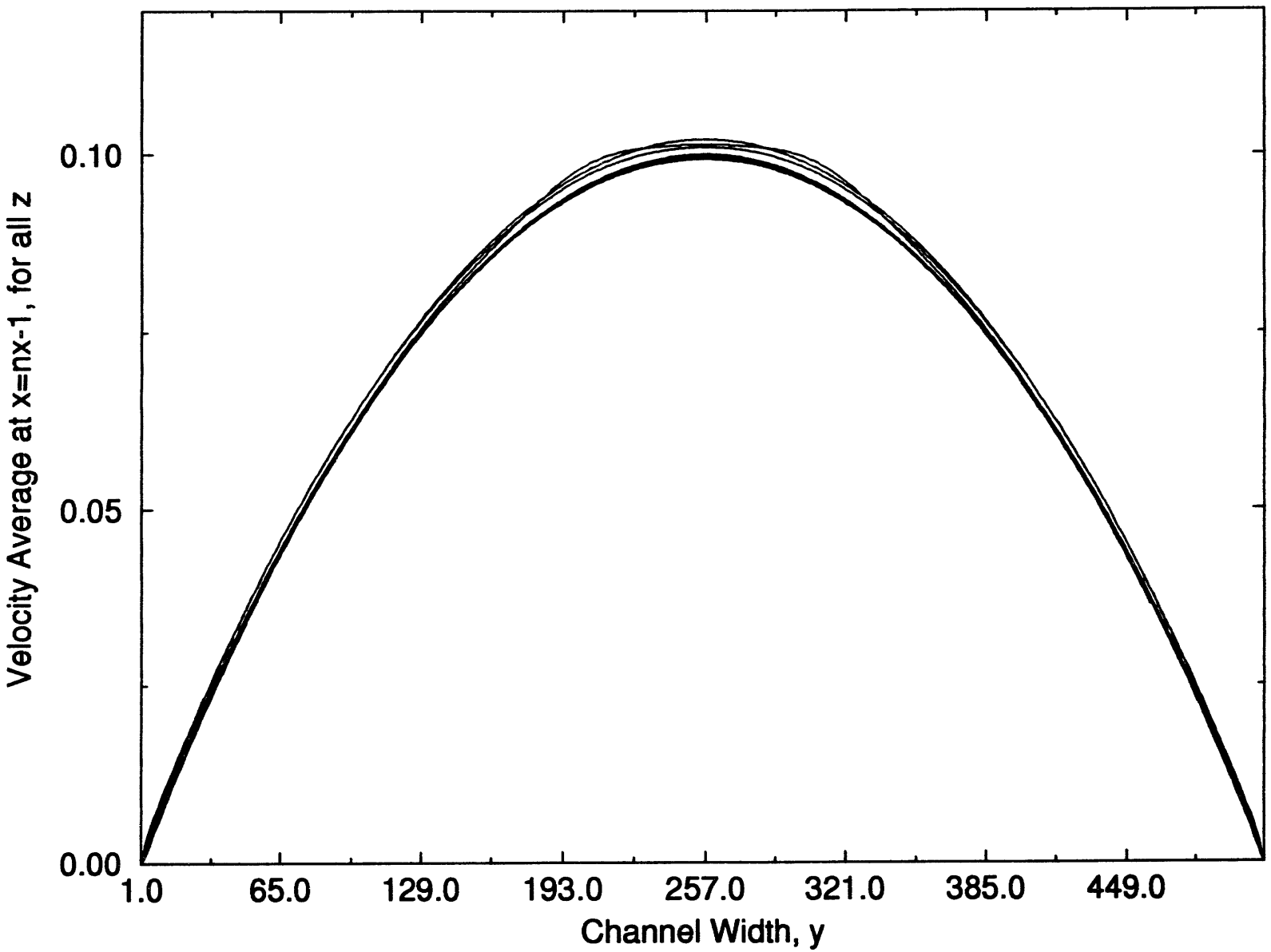

Transition to Turbulence in Channel Flow

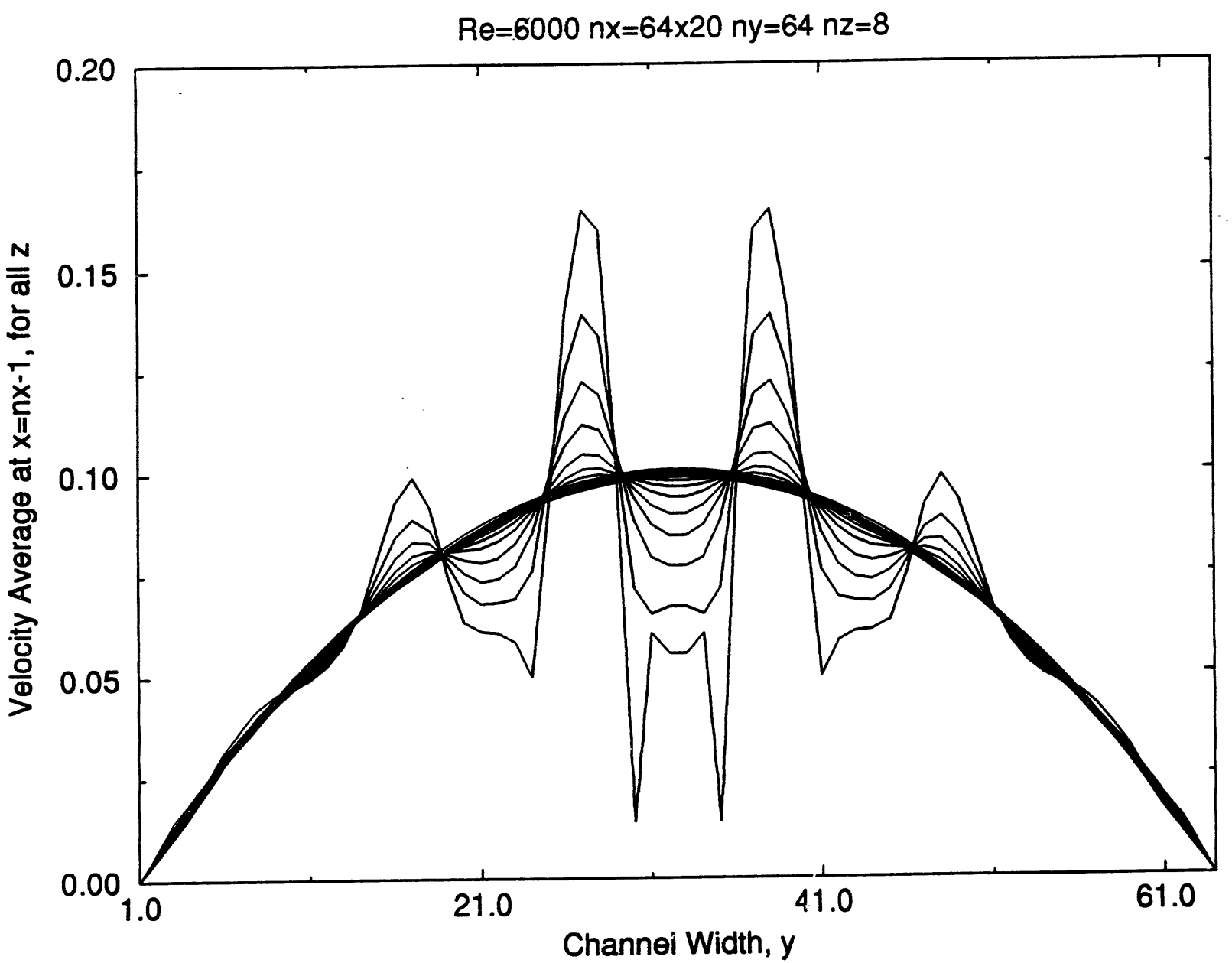

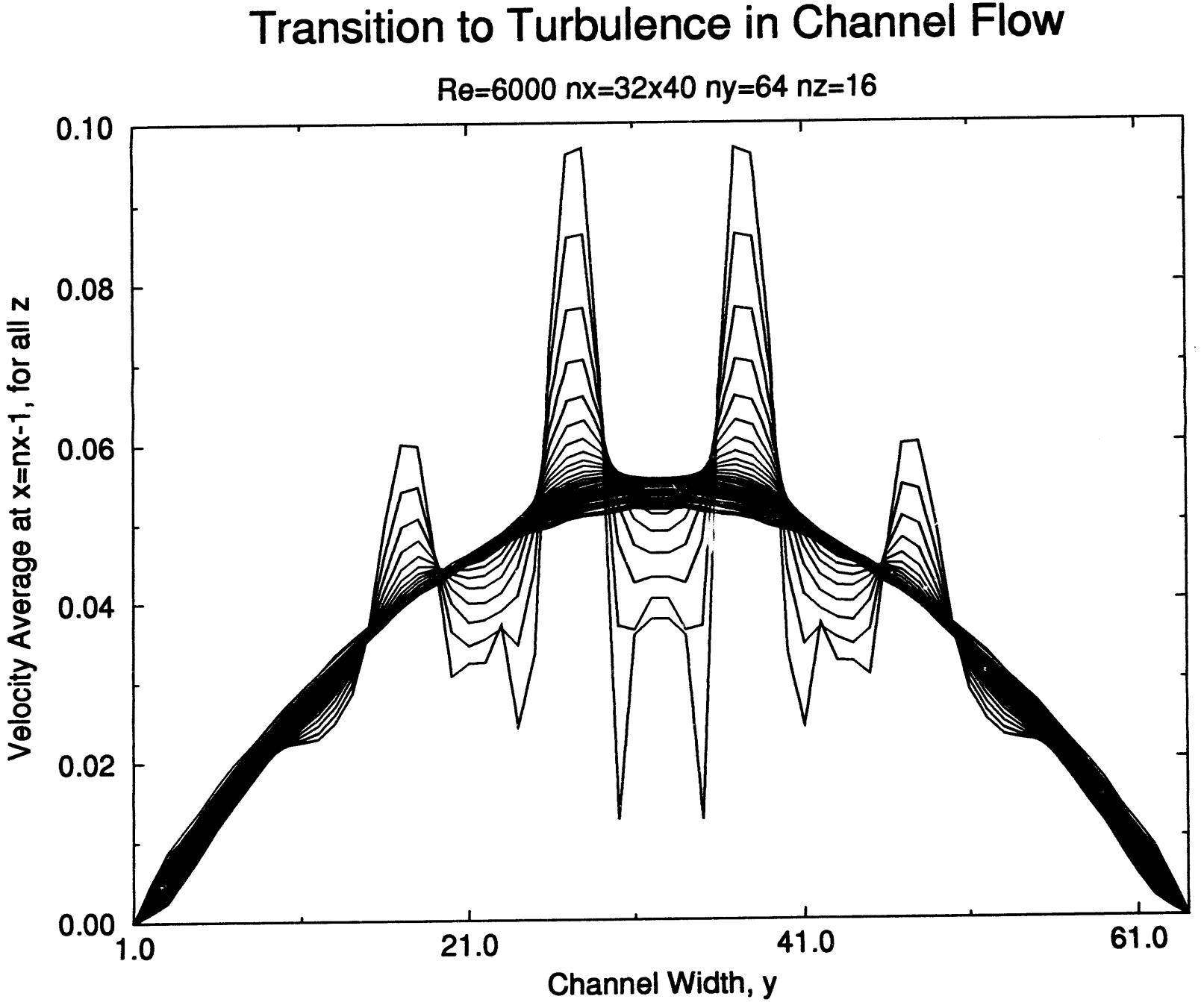
Transition to Turbulence in Channel Flow
Re=6000 nx=32x40 ny=64 nz=16
Velocity Average at x=nx-1, for all z
0.10
0.08
0.06
0.04
0.02
0.00
1.0
21.0
41.0
61.0
Channel Width, y

Chapter 4

Recommendations

In reference [2] Boris concludes that "a factor of two increase in the spatial resolution of (nonlinear monotone) models will bring more improvement in the accuracy of the well resolved scales than all the work in the world on the subgrid model of a more coarsely resolved LES model with the usual filtering procedure contaminating the long wavelengths unnecessarily." With such harsh criticism of LES models, it is recommended that future LB studies of simulating turbulent fluid flow focus on the stabilization of the methods for underresolved flow. (Alternatively, the instability may be considered to be a "good thing" because it indicates underresolution. Add grid points!) In a spirit similar to that of nonlinear monotone convection algorithms, we have proposed in Section 2.4 several methods that seek to stabilize short wavelength oscillations while seeking to avoid "contamination" of the long wavelengths.

Are there conditions under which LB schemes are already stable to even steep gradients? Recent work by Sterling and Chen [14] investigated the linear instability of uniform flows as a function of mean velocity, mass distribution parameter, the collision relaxation time, and the wavenumber. Stable parameter ranges were identified and in some cases all wavenumber were indeed stable for uniform flow. The introduction of velocity gradients into the analysis was not performed and simulations indeed become unstable when velocity gradients become large. It is recommended that entropy-increasing collisions be introduced to affect stability for sharp flow gradients as discussed in Section 2.4.

Bibliography

[1] Ugo Piomelli, William H. Cabot, Parviz Mion, and Sangsan Lee. Subgrid-scale backscatter in turbulent and transitional flows. *Physics of Fluids A*, 3:1766–1771, 1991.

[2] Jay Boris. Comment 1: On large eddy simulation using subgrid turbulence models. In *Wither Turbulence? Turbulence at the Crossroads*, 1989. Cornell University, Ithaca NY.

[3] W. G. Vincenti and Jr. C. H. Kruger. *Introduction to Physcial Gas Dynamics.* John Wiley and Sons, 1965.

[4] Hudong Chen, ShiYi Chen, and William H. Matthaeus. Recovery of the navier-stokes equations using a lattice-gas boltzmann method. *Physical Review A*, 45:R5339–5342, 1992.

[5] D.O.Martinez, W. H. Matthaeus, S. Chen, and D. C. Montgomery. A comparison of spectral methods and lattice boltzmann simulations of two-dimensional hydrodynamics. *submitted to Physics of Fluids A*, 1993.

[6] S. Klainerman and A. Majda. Compressible and incompressible fluids. *Commun. Pure Appl. Math.*, 35:629, 1982.

[7] L Kadanoff, G. McNamara, and G. Zanetti. Use of the boltzmann equation to simulate lattice-gas automata. *Physical Review A*, 40:4527, 1989.

[8] G. McNamara and G. Zanetti. Use of the boltzmann equation to simulate lattice-gas automata. *Phys. Rev. Lett.*, 61:2332, 1988.

[9] F. J. Alexander, S. Chen, and J. D. Sterling. Lattice boltzmann thermohydrodynamics. *Physical Review E*, 47:2249, 1993.

[10] Mario Ancona. Fully-langrangian and lattice-boltzmann methods for solving systems of conservations equations. *submitted to J. Comp. Phys.*, 1993.

[11] J. Smagorinsky. *Mon. Weather Rev.*, 91:99, 1963.

[12] Massimo Germano, Ugo Piomelli, Parviz Moin, and William H. Cabot. A dynamic subgrid-scale eddy viscosity model. *Physics of Fluids A*, 3:1760–1766, 1991.

[13] F. J. Alexander, S. Chen, and D. W. Grunau. Hydrodynamic spinodal decomposition: Growth kinetics and scaling functions. *Physical Review B*, 48:634–637, 1993.

[14] James D. Sterling and Shiyi Chen. Stability analysis of lattice boltzmann methods. ***submitted to** J. Comp. Phys.*, 1993.

DATE
FILMED
2/9/94
END